Paper presented at the 8th "European Symposium on Materials and Fluid Sciences in Microgravity", Bruxelles, April 1992

SINGLE BUBBLE EXPERIMENTS IN POOL BOILING
–
RESULTS FROM TEXUS 26

B.Vogel J. Straub
LATTUM, Technische Universität München
Arcisstr. 21, D-8000 München 2
Germany

Abstract

Due to the fact that heat transfer in pool boiling is a complex process, simplifying model experiments have been conducted in microgravity to render possible an insight into the details of the energy transport. For this purpose, specially developed spot heaters have been introduced to generate single bubbles, which in combination with conventional flat plate heaters guaranteed physically well based experiment conditions for pool boiling.

The measuring data of the heat fluxes were used as input data of an elaborate numerical simulation of temperatures in the heater and the fluid. Before onset of boiling (ONB), only heat conduction governs the energy transport, whereas after ONB the evaporation process has to be added to the model. The results were compared to measured heater temperatures and show very good agreement.

Based on video tape recordings, bubble growth rates have been extracted and compared to theoretical models as well as emperical correlations found for pool boiling in μg in literature. In principle the results coincide; the small deviations found may be explained by the specific setup of our heater arrangement.

The most interesting point of these experiments is the evaluation of interferometry images from the flight experiment. Due to axial symmetry of the phase object, Abel corrections had to be made for the calculation of the temperature profiles close to the bubbles. At the same time deflection of light was taken into account, which makes it possible to simulate the entire interferometer numerically.

The temperature profiles in combination with the numerical simulation of the heater distribution lead to the statement, that pool boiling under microgravity is mainly determined by the evaporation process itself. Secondary heat transport mechanisms in subcooled boiling are Marangoni convection due to temperature gradients along the bubbles.

Keywords: Pool Boiling, Single Bubble, Evaporation, Marangoni Convection, Numerical Simulations

1 Introduction

Although boiling is studied for more than 60 years, no theoretical model could be develloped covering the entire nature of this process. The individual models are only able to explain specific effects, but the main heat transfer mechanisms still seem not to be clear. This fact is also stressed by the surprising results gained in prior TEXUS and KC 135 experiments that boiling is independent from gravity, which is in contradiction to many theoretical models. To extract the dominat heat transfer mechanisms, detail experiments in microgravity are very useful, because disturbances due to natural convection are eliminated and evaporation can be observed almost directly.

2 TEXUS 26 Experiment Description

The experiment performed in TEXUS 26 should give an insight into the boiling phenomena around vapor bubbles. The main measuring instrument is an interferometic optics called differential or Schlieren interferometer. Since the evaluation of interferograms may become very complicated for complex experiments, the boiling process is studied at a single bubble. The interaction between the bubbles will be observed in a separate experiment to be planned later. Additionally, temperatures in the fluid at different locations, the fluid pressure and the heat input are measured with convectional techniques. A typical experiment cycle may be listed as follows:

- set fluid temperature
- set fluid pressure
- initiate bubble by using a spot heater
- control of heat flux
- shut off heater

Due to the limited time during a TEXUS flight, the fluid temperature was not changed during the flight itself, but was set to the desired value during countdown. For an optimal performance, a combined timer-telecommand control of the experiment was implemented, meaning, that the timer controlled the fluid pressure and switched on the heaters at predefined times. The PI had the opportunity to control the heat flux stepwise and to shut off heaters according to the experimental scenery on the TV monitor.

The μg- period was used for 7 different experiment cycles, eached followed by a rest phase to reach equilibrium again by a stirrer mechanism inside the cell. The cycles can be subdivided into the following groups:

- boiling with saturated fluid (1 cycle)
- boiling with subcooled fluid (3 cycles)

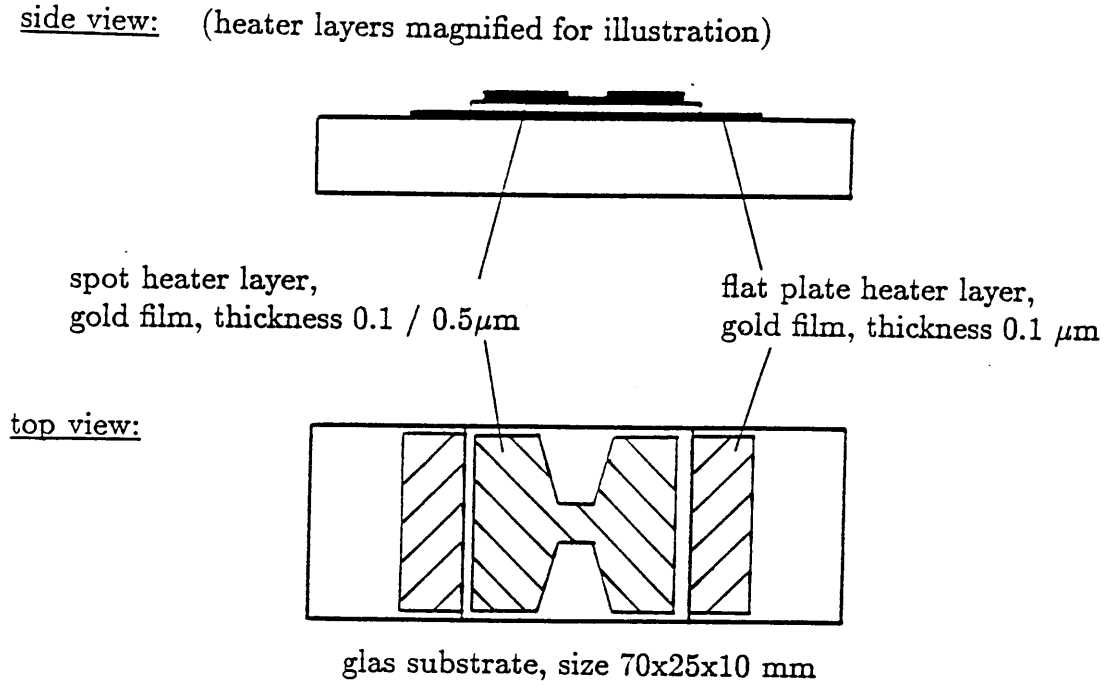

Figure 1: Sketch of the combined flat plate / spot heater

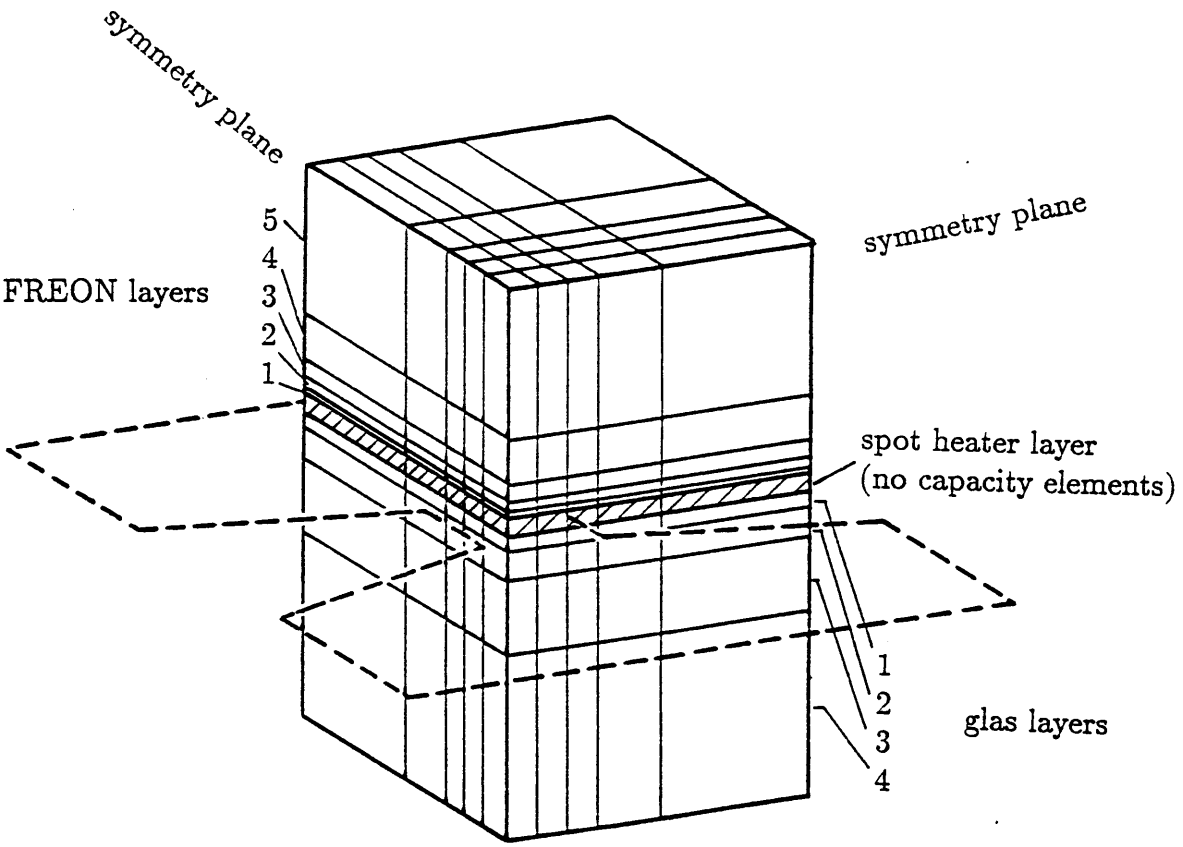

Figure 2: Finite element model of the heaters and the fluid

- boiling with system pressure variations (2 cycles)
- boiling during re-entry of the payload (1 cycle)

The experiment started with a saturated state and changed to a subcooled state during the second cycle. In the next three runs, subcooled boling was studied in respect to the influence of the temperature field close to the heater wall. To establish different temperature gradients, a flat plate heater beneath the spot heater was switched on a few seconds prior to the spot heater with different heat fluxes. Before re-entry, another cycle with pressure variation between two subcooled liquid states was performed to directly observe evaporation and condensation effects.

3 Evaluation of the experiment

3.1 Heater temperatures

For the generation of single bubbles, a special type of heater is required, because the usual flat plate heater does guarantee that bubbles generated in a single place. Therfore, a new heater type was designed, the so-called spot heater which has a typical shape (Fig. 1). The center part of the heater is narrow compared to the rest of the gold layer and its thickness is only 1/5. As a result, the resistance of the center is about 80% of the total spot heater resistance providing a means to establish a hot spot for nucleation without influencing the temperature fields at the edges. The flat plate heater, located below the spot heater, is used to set defined temperature gradients as well as for overall heating in pool boiling.

Two important parameters in boiling experiments are the heat flux imposed on the heater and the heater temperature. Since the gold layer used for heating are simple electrical resistors, both values can be determined by measuring the heater voltage and current. The temperature resistance relations of both heaters were measured prior to launch and afterwards in calibration runs. Since the resistance measured is an integal value over the entire heater, corrective calculations were needed to determine the spot heater temperature. The power distribution in the spot heater is not uniform in respect to area, as it is the case for the flat plate heater. Therefore, a numerical model was set up using finite element methods. Fig. 2 gives an impression of the distribution of calculation modes in the heater element.

Due to symmetry consideration, only one quarter of the glass substrate had to be modelled with the symmetry planes being adiabatic. The center of the spot heater was divided into four individual elements for a better numerical behavior of the algorithms. The size of the finite elements was chosen in respect to the anticipated temperature distribution and temperature gradients. The glass substrate consists of 4 layers of elements in the z-direction. The second glass substrate layer is also used for thermally representing the flate plate heater.

An additional layer for this heater would not influence the results, but slow down calculation speed. The fluid (FREON 113, a thermal insulator in respect to its properties) was modelled with 5 different layers of individual thickness. The input data for the calculations were the measured, therefore time-dependent heat fluxes for both heaters and the initial temperatures, which were assumed to be constant over the calculation area. These assumptions can be validated by calculating the equilibration process after each experiment cycle, at least for the first five ones. The heat flux distribution is uniform in respect to the area for the flat plate heater. For the spot heater, the input energy was distributed according to precalculated local temperatures. So, approximately 80% of the spot heater energy is imposed on the center, which caused numerical problems in the beginning. The calculated center temperatures are compared with the evaluated measurement data in fig. 3. Cycle 5 is omitted here because of the missing measurements. As it can be clearly observed, the calculations are in good agreement with the measurements, especially in the first experiment run, in which the condition of equilibrium at start time is fulfilled the best.

In runs 6 and 7, characteristic deviations just after heater activation can be recognized. They are definitely due to the non uniform temperature distribution at the very center in the beginning of the calculations. Nevertheless, calculations and measurements meet after some seconds, when the system behavior is governed by the heat input and not by the initial conditions.

3.2 Bubble Growth under μ-gravity

Since the lack of buoyancy forces strongly influences the boiling regime, it is of special interest to examine bubble growth under microgravity. For pool boiling on earth, there are many publications which deal with this aspect for different fluids and heater configurations. A comparison of the selected publications will be made at the end this chapter.

From publications of Straub, Zell and Vogel (1989), (1990), it is known that bubble sizes increase for a pool boiling system under microgravity by a factor 3...8. Zell (1991) evaluated movie film from an experiment on TEXUS 8 and found that the diameter of the growing bubble changes with time according to the following law:

$$d_{bubble}(t) = c \cdot Ja\sqrt{a_l \cdot t} \quad \text{and c} = 0.62 \qquad (1)$$

The same type of function was proposed by Plesset and Zwick (1954) for water at atmospheric pressure for pool boiling on earth. A characteristic difference between bubble growth on earth and under microgravity is, however, that the time scales are completely different. In the first case, bubble growth ends with the departure from the heater in some ten milliseconds, whereas in the latter case the end is given at the moment the growing bubble coalesces with surrounding bubbles in some tenth of a second.

For single bubble experiments, a definite end of bubble growth can not be given, because the natural coalescence mechanism for μg is suppresses by the experiment setup. But here as well, after one or two seconds, a steady state in the bubble dimension is reached at least for subcooled boiling, when evaporation at the heater wall and condensation at the bubble cap are in equlibrium.

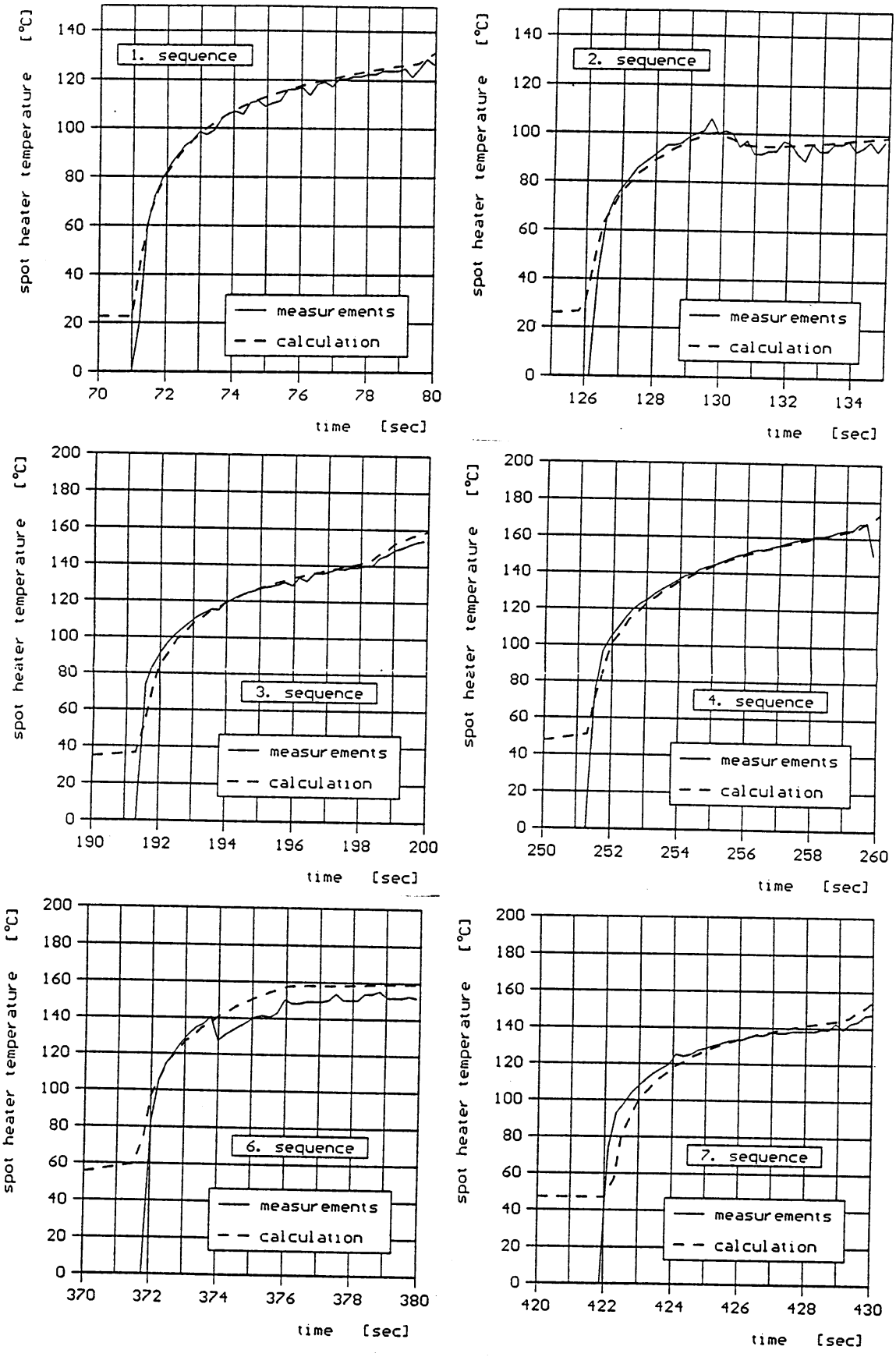

Figure 3: Spot heater temperatures

Due to the large time scale, the acquisition rate of the video system (25 fps) was sufficient for a detailed analysis, although a higher rate would have been preferable for the initial bubble growth.

Three experimental cycles were suitable for bubble growth rate evaluation. Fig. 4 illustrates one example; it can be clearly seen that the bubble is nearly spherical, allowing a very simple calculation of the bubble volume. The bubble diameter and its height is measured using a digital image processing system. Applying the above mentioned information, a sphere adequate bubble radius is calculated and can be plotted versus time (fig. 5). The corresponding curves are added in fig. 4. The analysis of initial bubble growth might also imply different relations, but the video frequency was to low to confirm this behavior with a higher degree of accuracy.

To establish a correlation analog to Zell, the wall superheat has to be taken into account. To determine the corresponding Jakob numbers Ja, results of the numerical calculations of the temperatures inside the heater were used. These results were used due to the nonuniform temperature distribution in the spot heater, in contrast to Zell who measured average heater temperatures.

The evaluation of bubble size was stopped, if bubble dimensions exceded the visible part of the experimental volume. This occured in the first evaluated sequence at a calculated radius of $R_{max} = 5.95mm$ due to the low subcooling. In the two other experiment runs the maximum radius is almost equal to the steady state value, which would have been reached for unlimited experimental time.

Regression analysis of the data showed that bubble growth for these single bubble experiments could be represented best with the relation

$$R(t) \sim t^{1/3} \tag{2}$$

over the entire time scale.

These Jakob Numbers apply the best for an analysis of subcooling with 4.5 K given

$$R(t) = 0.54 \cdot Ja\sqrt{a_l} \cdot t^{1/3} \quad \text{with Ja} = 32 \tag{3}$$

and for a subcooling of 26 K:

$$R(t) = 0.091 \cdot Ja\sqrt{a_l} \cdot t^{1/3} \quad \text{with Ja} = 92 \tag{4}$$

$$R(t) = 0.091 \cdot Ja\sqrt{a_l} \cdot t^{1/3} \quad \text{with Ja} = 110 \tag{5}$$

To extract a common behavior concerning the subcooling or the reduced pressure p/p_c would not be justified due to the limited number of experiment runs.

3.3 The heat transport mechanisms

One of the most important questions in microgravity boiling concerns the near range temperature field of bubbles either for saturated or subcooled liquid state. The temperature field around the bubble on the heater side is determined by the primary heat transfer from the heater wall by evaporation. Analogous to this, do the secondary heat transfer mechanisms control the temperature field on the opposite side - the bubble cap. A schematic diagram of a vapor bubble at the heater wall is given in fig. 6: here, an effort is made to separate the different heat transport mechanisms from each other and to postulate the influence region for each of them. The energy path via the microfilm will be very limited in its duration, because shortly after onset of boiling, bubbles stick to the heater very closely, and a existing microlayer dries out very quickly. Since the test cell could not be temperature controlled during the count-down, the saturated fluid was not reached. However, a comparison of the different subcooling procedures can be made instead. During bubble growth more liquid is evaporated at the bubble base than vapor condensates at the bubble cap until equilibrium is reached and the bubble size remains constant. Simultaneously, surface tension convection may develop along the vapor liquid interface. In the case of single bubbles, this would adequately describe the process for μg, for a realistic regime bubble coalescence needs to be added. Small bubbles grow in the vicinity of large bubbles and coalesce with these promoting the mass flow through the larger bubbles.

The first area of interest has been the bubble base. Although the bubble dimensions in μg are more suitable for an analysis, it was not possible to obtain information about the temperature field at the triple interface heater vapor liquid due to the kinetics of boiling and the comparatively low video picture rate of 25 fps and additional light deflection at the heater wall. For these investigations dual recording with video and movie as well as technical rough heater surfaces would be required.

The numerical simulation, however, lead to the statement that evaporation play a major role in this area. During the very first moments of bubble life, any existing microlayer is dried out. Later, fluid being close to the triple interface heater vapor liquid is evaporated directly into the bubble. From ealier TEXUS flights it is known that also bubble coalescence between new small bubbles and already existing large bubbles can be regarded as a way of transferring energy to the large bubbles.

The second area of interest, the bubble cap, was evaluated for several conditions: boiling at low subcooling, boiling at high subcooling, recondensation and boiling with superimposed Marangoni flow. For the first three cases a few characteristics can be summarized: it is assumed that the vapor inside the bubble is the saturation temperature or close above due to the small dynamic excess pressure. The ambient liquid temperature has been measured with thermocouples. Both temperatures present the limits of the thermal boundary layer of the bubbles. In all cases the thermal boundary layer is very thin, which caused some problems at the start of the evaluation. These difficulties were overcome by introducing a basic temperature profile function around the bubble, which had been found by a comparison of calculated pictures using a different model functions with original flat images. For the temperature field, the following relation in respect to the radius was used:

$$T(r) = T_\infty + (T_{sat} - T_\infty) \cdot 1/2^{\frac{(r-D/2)}{L}} \tag{6}$$

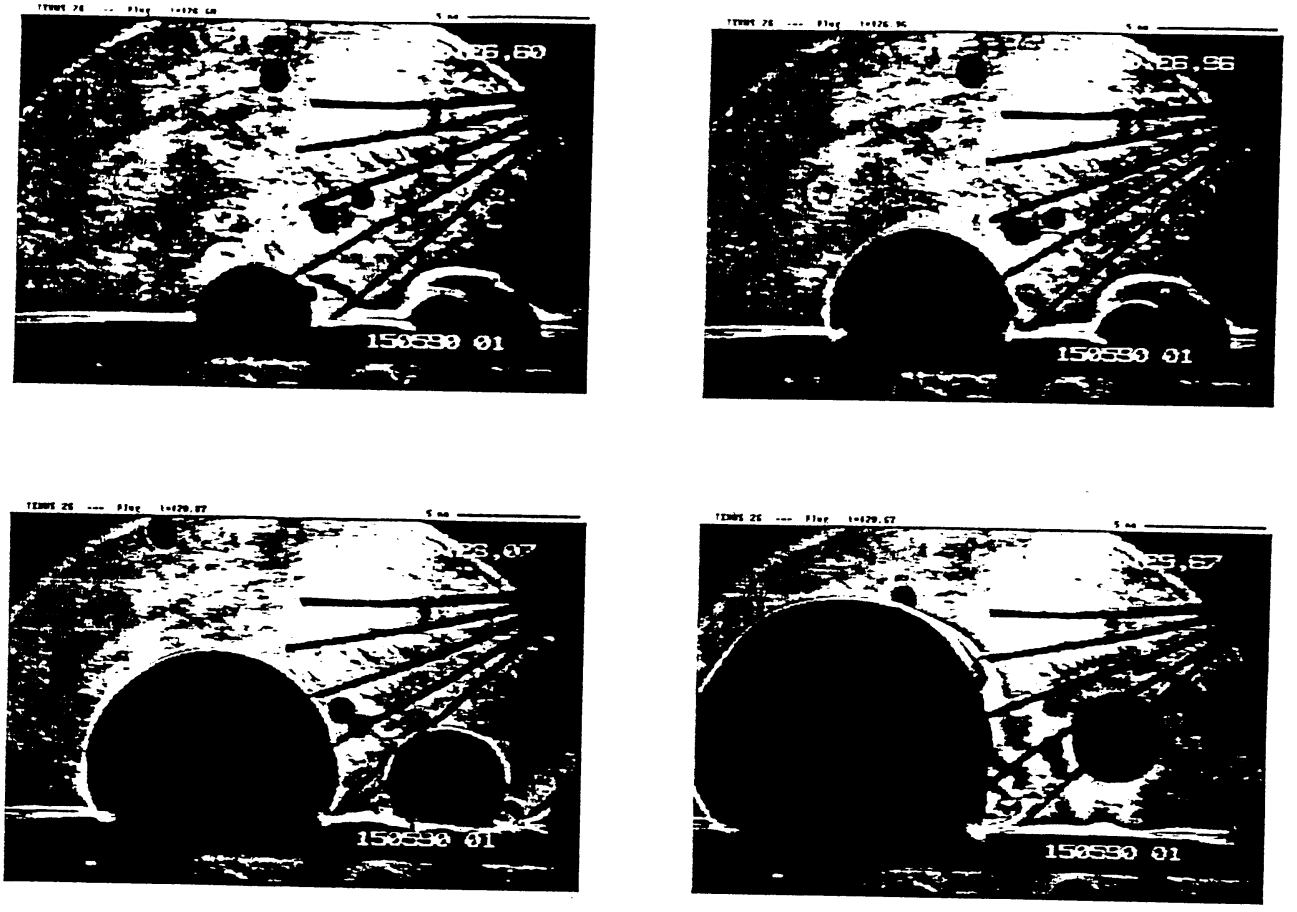

Figure 4: Bubble growth under microgravity

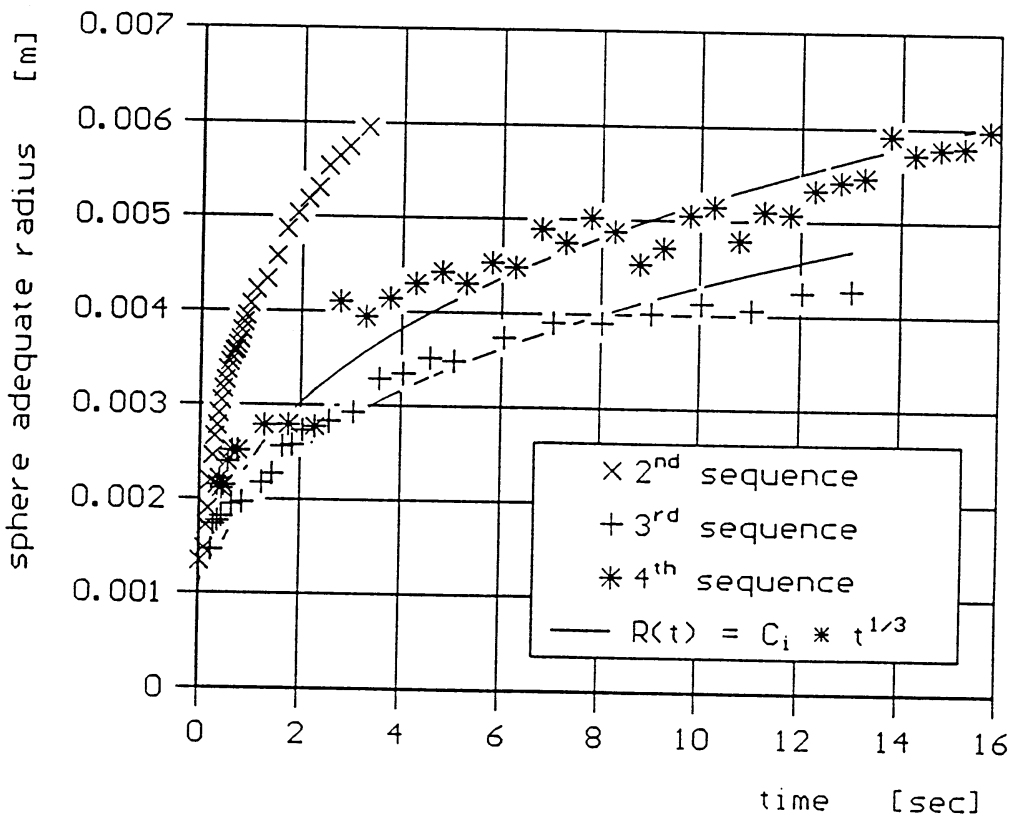

Figure 5: Calculated sphere adequate bubble radii for different subcooling rates

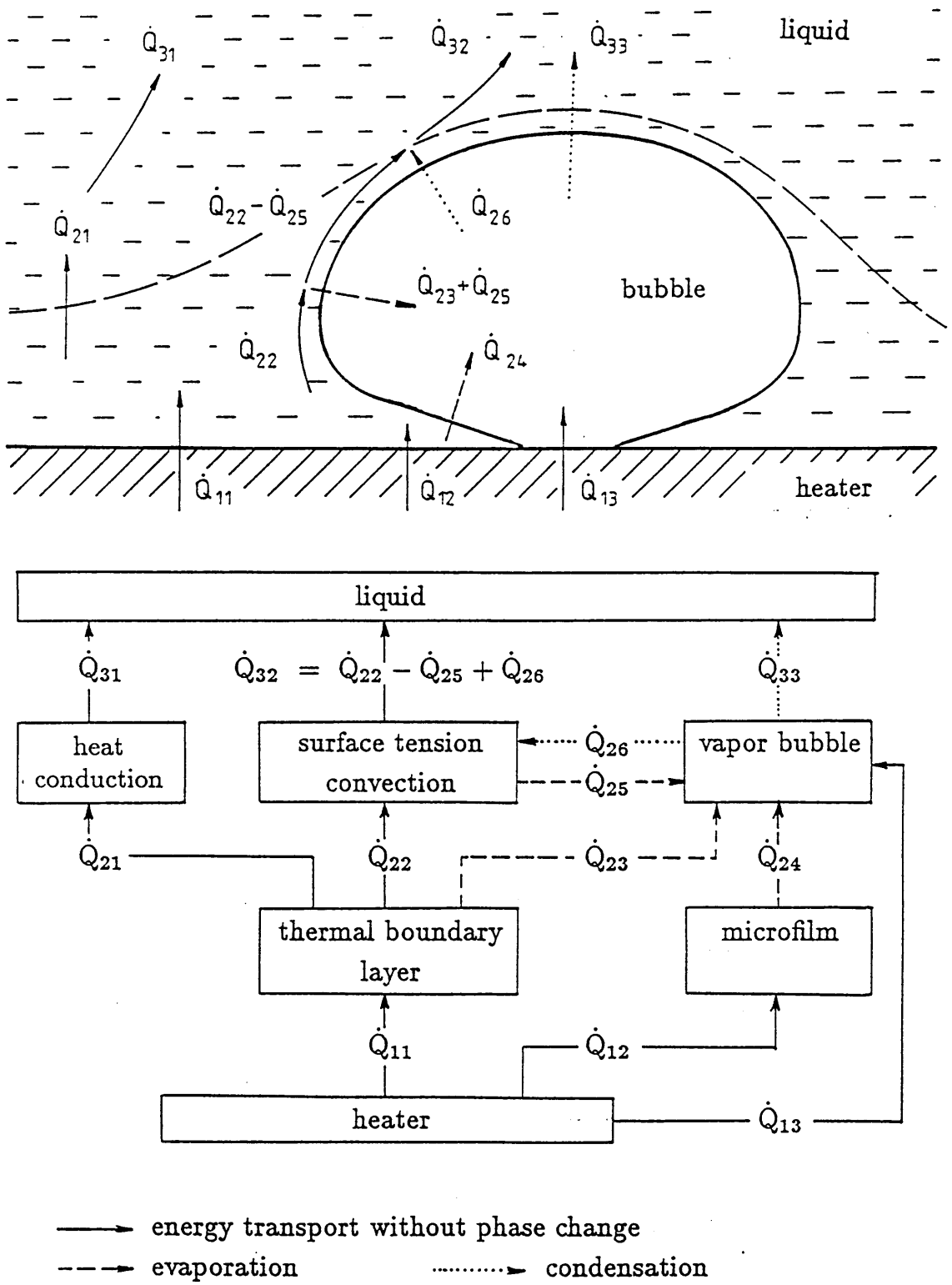

Figure 6: Schematic sketch of boiling heat transfer under μg

with $T_{sat} - T_{\infty}$ being the driving temperature difference, D the bubble diameter and L the length scale, which has to determined for each picture to be evaluated. A general law for the dependencies of L on subcooling and bubble size can not yet be given due to the limited number of experiment runs. The order of magnitude for the relation L/R_{Bubble} is in the order of 0.01 to 0.1. The influence area of the bubble on the temperature field is very small and limited to a thin boundary layer.

A completely different situation is given if Marangoni flow exists as a secondary heat transfer mechanism. Here the interferometer fringes from a chimney reaching from the bubble cap deep into the bulk liquid. The diameter of this chimney is close to the bubble diameter and the height is usually larger than the observable experiment volume. Based on our experiments with KC 135 flights at NASA, it is known that the extension of this chimney may be in order of 6...10 bubble diameters for selected fluid states. Velocities close to the vapor liquid interface are currently being measured in reference experiments on the ground.

Condensation in combination with surface tension flow is responsible for the transport of energy from the vapor bubbles further on into the bulk liquid. Detailed calculations about the transferred amounts of energy are in progress.

4 Conclusion

The TEXUS flight showed that single bubble experiments are very useful for determining heat transport mechanisms in pool boiling. In a series of experiment runs in subcooled boiling, data about bubble growth, heater temperature distributions and temperature profiles close the bubble were gained and evaluated. As a result it can be stated that the main heat transport mechanism is evaporation at the heater wall. Condensation together with Marangoni flow serve as secondary mechanisms for the heat transport from the vapor bubble further on into the bulk liquid.

Acknowledgement

This project was founded by the German space agency DARA, Bonn. We thank all people involved in the project management of BMFT and DARA, and all members of the TEXUS teams of MBB/ERNO, Kayser–Threde and MORABA/DFVLR for their support. They all contributed to the success of this experiment on TEXUS 26.

References

[1] Chen, Y. M.: *Wärmeübergang an der Phasengrenze kondensierender Blasen*, Ph.D. thesis, Technische Universität München, 1985

[2] Fritz, W.: *Berechnungen des Maximalvolumens von Dampfblasen* , Phys. Z. 36, pp. 379–384, 1935

[3] Goldstein, R.J.: *Optical Measurement of Temperature* ; in Measurements in Heat Transfer, edited by E.R.G. Eckert and R.J. Goldstein, 1976

[4] Hauf, W.; Grigull, U.: *Optical Methods in Heat Transfer*, Advances in Heat Transfer, Vol. 6, pp 133–366, 1970

[5] Judd. R.L.; Merte, H. jr.: *Evaluation of Nucleate Boiling Heat Flux at Varying Levels of Subcooling and Acceleration* Int. Journal Heat and Mass Transfer, Vol. 15, pp.1075–1096, 1972

[6] MBB/ERNO: *TEXUS 25/26 Flight Implementation Plan and Experiment Interface Specification* MBB/ERNO, Bremen, part VI, 1990

[7] Memmel, R.; Straub, J.: *Differentialinterferometrie; in Optische Meßmethoden in der Wärme- und Stoffübertragung, edited by F. Mayinger, München, 1991*

[8] Plesset, M.S.; Zwick, S.A.: The Growth of Vapor Bubbles in Superheated Liquids; J. Applied Phys. 25, (1954), pp. 493–500, 1954

[9] Stephan, K.; Abdelsalam, M.: Heat Transfer Correlations for Natural Convection Boiling; Int. J. Heat Mass Transfer 23, pp. 73–87, 1980

[10] Straub, J.; Zell, M., Vogel, B. Pool Boiling in a Reduced Gravity Field; Proc. 9th Int. Heat Transfer Conf., Jerusalem 1990

[11] Zell, M.; Straub, J., Vogel, B.: Pool Boiling Under Microgravity; J. PhysicoChemical Hydrodynamics, Vol. 11, No 5/6, pp 813–823, 1989

[12] Zell, M. Untersuchung des Siedevorgangs unter reduzierter Schwerkraft; Ph.D. thesis, Technische Universität München, 1991